A multigrid method based on cell orientated discretization for convection-diffusion problems

Dietmar Hietel and Jürgen Witzel

Arbeitsgruppe Numerische Mathematik
Technische Hochschule Darmstadt
Schloßgartenstraße 7, 64289 Darmstadt

Dedicated to Willi Törnig on the occasion of his 65th birthday

Abstract

For the convection-diffusion equation in two dimensions we derive the cell orientated discretization which is based on the method of lines leading to differential-algebraic equations and their time integration by implicit methods. This approach is well-suited in convection-dominated cases. The efficiency of the method depends on the solution of the arising linear systems mainly. Motivated by the definiteness properties of these unsymmetric systems we choose a multigrid method with problem adapted transfer operators. The interpretation of the cell orientated discretization in a finite-volume or a Petrov-Galerkin context leads to different definitions of restriction and prolongation. In combination with smoothers which are exact solvers in the convection case (Gauss-Seidel, ILU) we achieve a robust multigrid iteration. Finally we present numerical results concerning the quality of the transfer operators as well as the various smoothing iterations. The independance of the convergence rate from the gridsize and the behaviour of various time integration schemes are also examined.

1 Introduction

As a model problem for the derivation of our discretizations we consider the unsteady linear convection-diffusion equation of the form

$$u_t + Lu = q \quad \text{with} \quad Lu = \boldsymbol{\nabla} \cdot (\boldsymbol{\beta} u - \epsilon \boldsymbol{\nabla} u) \tag{1}$$

on a bounded domain $\Omega \subseteq \mathbb{R}^2$ with constant diffusion coefficient $\epsilon > 0$ and a given divergence free velocity field $\boldsymbol{\beta}(\boldsymbol{x})$ in $\mathbb{R}^2$. The initial and boundary conditions are given by

$$\begin{array}{rcll} u(\boldsymbol{x},0) & = & u_0(\boldsymbol{x}) & \text{on} \quad \Omega \\ u(\boldsymbol{x},t) & = & u_D(\boldsymbol{x}) & \text{on} \quad \Gamma_D \supseteq \Gamma_{\text{in}} := \{\boldsymbol{x} \in \partial\Omega\,,\ \boldsymbol{\beta}(\boldsymbol{x}) \cdot \boldsymbol{n} \leq 0\} \\ \partial_n u(\boldsymbol{x},t) & = & 0 & \text{on} \quad \Gamma_N \subseteq \partial\Omega \setminus \Gamma_D\,. \end{array} \tag{2}$$

In the convection dominated case ($|\boldsymbol{\beta}| \gg \epsilon$) boundary layers can occur due to Dirichlet conditions on the outflow boundary if $\Gamma_D \setminus \Gamma_{in} \neq \emptyset$ and internal layers have to be considered when using nonsmooth Dirichlet data u_D.

The cell orientated discretization is based on the method of lines and an appropriate treatment of the space operator L. This approach is well suited for problems arising in the convection dominated case even when using coarse grids with high Péclet number $\mathrm{Pe} = h|\boldsymbol{\beta}|_{\max}/\epsilon$. The derivation of the semidiscretization and its implicit time-integration leading to the cell orientated discretization are described in the next section. Afterwards we study the properties of the resulting linear systems.

The efficiency of the whole method is essentially influenced by the computational effort for solving the linear systems. In the case of a self-adjoint elliptic operator L the multigrid approach leads to an efficient solver. Therefore a multigrid method should work for diffusion dominated problems. For the convection equation ($\epsilon = 0$) the linear systems can be written in triangular form with a numeration adapted to the velocity field. Thus, the Gauss-Seidel or ILU iteration are fast solvers in convection dominated situations. For the development of a robust multigrid method we combine the multigrid idea with these iteration methods as smoothers. A main component to get a reliable multigrid algorithm is the specification of problem dependent restriction and prolongation operators. The multigrid method is described in section 3.

Finally numerical results concerning the quality of our discretization and the expected behaviour of the multigrid algorithm are presented.

2 Cell orientated discretization

The convection-diffusion equation (1) is a parabolic conservation law which can be written in integral form as one possibility of a weak formulation

$$\frac{d}{dt}\int_{\tilde{\Omega}} u\,dV + \oint_{\partial\tilde{\Omega}} [\boldsymbol{\beta}\cdot\boldsymbol{n}\,u - \epsilon\,\partial_n u]\;ds = \int_{\tilde{\Omega}} q\,dV \quad \text{for all } \tilde{\Omega} \subseteq \Omega \tag{3}$$

where $\tilde{\Omega}$ is a domain with piecewise smooth boundary $\partial\tilde{\Omega}$.

2.1 Semidiscretization

The cell orientated semidiscretization is based on a finite volume approach for (3) using the method of lines. This semidiscretization is introduced and described in detail in [5]. In the following we will outline the main steps of its derivation under the simplifying assumption of a constant velocity field $\boldsymbol{\beta}$ with nonvanishing components.

For a rectangular cell V with edges S_i (see fig 1) (3) leads to

$$\frac{d}{dt}\int_V u\,dV + \sum_{i=1}^{4}\boldsymbol{\beta}\cdot\boldsymbol{n}_i\int_{S_i} u\,ds - \epsilon\int_{S_i}\partial_n u\,ds = \int_V q\,dV\,. \tag{4}$$

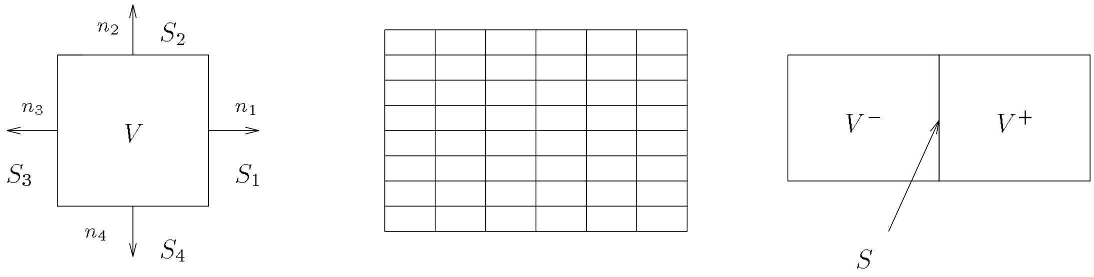

Figure 1: local cell, grid and neighbouring cells

Equation (4) motivates the use of average values of u and their semidiscrete analogues

$$
\begin{aligned}
u_V &\approx & u(V) &:= \frac{1}{|V|}\int_V u\,dV && \text{(cell average)}\,,\\
u_S &\approx & u(S) &:= \frac{1}{|S|}\int_S u\,ds && \text{(edge average)}\,,\\
\partial_n u_S &\approx & \partial_n u(S) &:= \frac{1}{|S|}\int_S \partial_n u\,ds && \text{(edge average of normal derivatives)}
\end{aligned}
\tag{5}
$$

where $|V|$ and $|S|$ indicate the measure of V and S, respectively.

For a rectangular grid with cells $V \in \mathcal{V}$ and edges $S \in \mathcal{S}$ (see fig 1) the finite volume equation (4) has for all $V \in \mathcal{V}$ the semidiscrete counterpart

$$
|V|\frac{d}{dt}u_V + \sum_{i=1}^{4}|S_i|\,[\boldsymbol{\beta}\cdot\boldsymbol{n}_i\,u_{S_i} - \epsilon\partial_n u_{S_i}] \;= |V|q_V\,. \tag{6}
$$

Here, q_V denotes the exact evaluation of $q(V)$ or for practical purposes an approximation by a cubature formula. Rewriting the boundary conditions in the form

$$
\begin{aligned}
u_S(0) &= u_D(S) && \text{for} \quad S \in \partial\mathcal{S}_D := \{S \in \mathcal{S} : S \subseteq \Gamma_D\}\,,\\
\partial_n u_S(0) &= 0 && \text{for} \quad S \in \partial\mathcal{S}_N := \{S \in \mathcal{S} : S \subseteq \Gamma_N\}
\end{aligned}
\tag{7}
$$

we get an underdetermined system. Thus we have to define additional conditions for edge averages u_S, $\partial_n u_S$. In finite volume methods u_S and $\partial_n u_S$ are substituted by a linear combination of cell averages in the neighbourhood of S so that they are formulated usually in terms of the cell averages only.

In contrast to this explicit flux representation we use an implicit one given by the representation of the normal derivative $\partial_n u_S$ in a cell V as a linear combination of the local averages

$$
\partial_n u_S = \alpha_V u_V + \sum_{i=1}^{4}\alpha_{S_i}u_{S_i}\,. \tag{8}
$$

The coefficients are determined by postulating the validity of (8) on a local trial space

$$
\mathcal{S}_V = \operatorname{span}\Big\{1, x_1, x_2, \exp\Big(\frac{\beta_1}{\epsilon}x_1\Big), \exp\Big(\frac{\beta_2}{\epsilon}x_2\Big)\Big\} \tag{9}
$$

containing the exponential functions as homogeneous solutions of the steady convection-diffusion equation (1) and all polynomials of degree 1. This choice enables the elimination of the normal derivatives in (6) and (7).

For each interior edge S belonging to two cells V^+, V^- (see fig 1) the normal derivatives $\partial_n u_S$ only have different signs so that we get additional constraints in terms of the unknowns $\vec{u}_{\mathcal{V}} := (u_V)_{V\in\mathcal{V}}$ and $\vec{u}_{\mathcal{S}} := (u_S)_{S\in\mathcal{S}}$ only. These equations combined with the finite volume equations (4) and boundary conditions altered by the elimination of the normal derivatives define a differential-algebraic system of the form

$$\boldsymbol{M}\frac{d}{dt}\vec{u} + \boldsymbol{B}\vec{u} = \vec{b} \iff \begin{pmatrix} \boldsymbol{V} & 0 \\ 0 & 0 \end{pmatrix} \frac{d}{dt} \begin{pmatrix} \vec{u}_{\mathcal{V}} \\ \vec{u}_{\mathcal{S}} \end{pmatrix} + \begin{pmatrix} \boldsymbol{B_{11}} & \boldsymbol{B_{12}} \\ \boldsymbol{B_{21}} & \boldsymbol{B_{22}} \end{pmatrix} \begin{pmatrix} \vec{u}_{\mathcal{V}} \\ \vec{u}_{\mathcal{S}} \end{pmatrix} = \begin{pmatrix} \vec{b}_1 \\ \vec{b}_2 \end{pmatrix} \tag{10}$$

where $\boldsymbol{V} = \mathrm{diag}(|V|)_{V\in\mathcal{V}}$.

Similarly to finite element methods the stiffness matrix $\boldsymbol{B}$ can be generated by cell matrices acting only on the variables of one cell.

2.2 Interpretation as a Petrov-Galerkin method

In the preceding subsection we have given a derivation of the semidiscretization as a finite-volume-type method under the assumption of constant velocity field $\boldsymbol{\beta}$. In view of the extension to a variable velocity field $\boldsymbol{\beta}(\boldsymbol{x})$ it is helpful to formulate (10) as an equivalent Petrov-Galerkin method. In the one-dimensional case this leads to a conforming, and in two dimensions to a nonconforming method.

In one dimension the weak formulation of (1) utilizing test functions reads for homogeneous Dirichlet data:

$$\text{Find } u \in H^1_E(\Omega):\ (u_t,\psi) + \epsilon(u_x,\psi_x) + \beta(u_x,\psi) = (q,\psi) \text{ for all } \psi \in H^1_E(\Omega)\,. \tag{11}$$

Here, $(\phi,\psi) = \int_\Omega \phi\psi\, dx$ denotes the L_2-scalar product associated with an interval Ω and $H^1_E(\Omega)$ is the Sobolev space $H^1(\Omega)$ with the essential (Dirichlet) boundary conditions. In contrast to finite element methods the specification of different subspaces of $H^1_E(\Omega)$ for the trial and test functions defines a conforming Petrov-Galerkin method. For a cell $V = (x_{j-1}, x_j)$ the local trial space $\mathcal{S}_V$ and test space $\mathcal{T}_V$ are – in analogy to (9) – given by

$$\mathcal{S}_V = \mathrm{span}\{1, x, \exp\left(\frac{\beta x}{\epsilon}\right)\} \quad \text{and} \quad \mathcal{T}_V = \mathrm{span}\{1, x, \exp\left(-\frac{\beta x}{\epsilon}\right)\}\,.$$

The exponential function $\phi = \exp(\frac{\beta x}{\epsilon})$ is a solution of the homogeneous equation $L\phi = 0$ whereas $\psi = \exp(-\frac{\beta x}{\epsilon})$ fulfills the adjoint problem $L^*\psi = 0$. In the limit case $\beta = 0$ we get by continuation from (11) $\mathcal{S}_V = \mathcal{T}_V = \mathrm{span}\{1, x, x^2\}$, which defines a Galerkin approach for this self-adjoint problem.

Using nodal values $\phi_j = \phi(x_j)$, $j \in \mathcal{J}$ and $\phi_V = \phi(V)$ the nodal basis of $\mathcal{S}$ reads

$$\mathcal{S} = \mathrm{span}\{\phi^j(x), j \in \mathcal{J}, \phi^V(x), V \in \mathcal{V}\}\,. \tag{12}$$

Similarly we can derive a nodal basis for

$$\mathcal{T} = \text{span}\{\psi^j(x), j \in \mathcal{J}, \psi^V(x), V \in \mathcal{V}\}\,. \tag{13}$$

The nodal functions for the self-adjoint and a convection dominated example are shown in fig 2. Approximating the evolutionary term and the right hand side of (11) by the sums

$$(u_t, \psi) \approx \sum_{V\in\mathcal{V}} |V| u_t(V)\psi(V) \quad , \quad (q, \psi) \approx \sum_{V\in\mathcal{V}} |V| q_V \psi(V) \tag{14}$$

we obtain the semidiscrete system in form (10).

Remark 2.1 The approximations (14) can be interpreted as lumping of the mass matrices consisting of the inner products (ϕ, ψ) for the nodal functions $\phi \in \mathcal{S}$ and $\psi \in \mathcal{T}$.

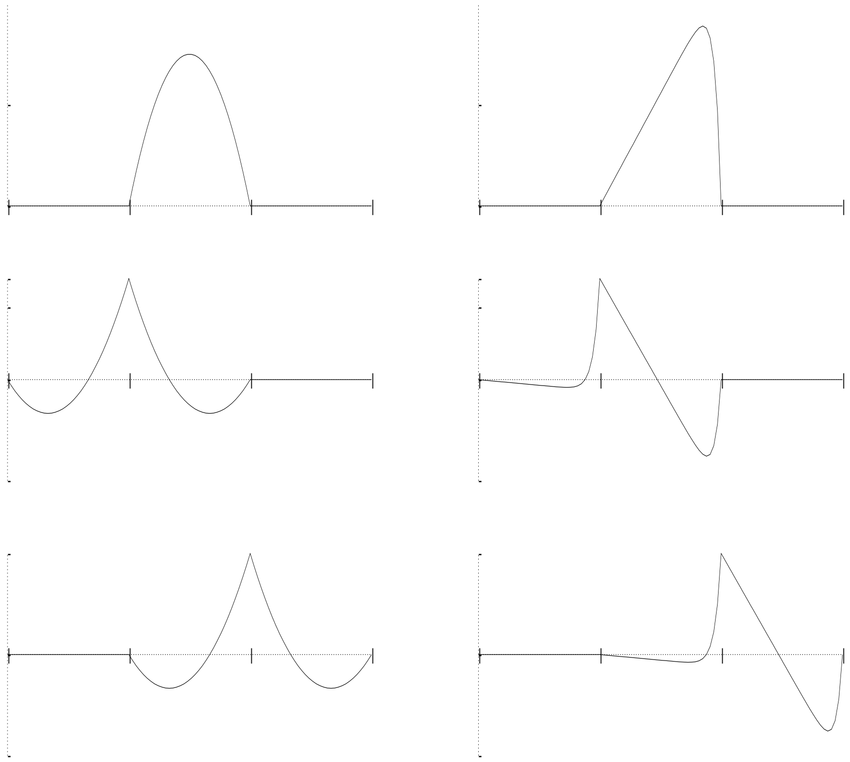

Figure 2: Trial functions for Pe=0 and Pe=10

In the 2D-case the local trial and test spaces are defined by

$$\begin{aligned}
\mathcal{S}_V &= \text{span}\{1, x_1, x_2, \exp\left(\frac{\beta_{V,1}x_1}{\epsilon}\right), \exp\left(\frac{\beta_{V,2}x_2}{\epsilon}\right)\} \\
\mathcal{T}_V &= \text{span}\{1, x_1, x_2, \exp\left(-\frac{\beta_{V,1}x_1}{\epsilon}\right), \exp\left(-\frac{\beta_{V,2}x_2}{\epsilon}\right)\},
\end{aligned}$$

where $(\beta_{V,i}) \approx \beta_i(V)$ are local approximations in case of variable velocity. We can derive an analogous representation to the trial space (12) and the test space (13) with the cell averages and the edge averages from (5) as nodal values. This means that the nodal functions are not continuous at interior edges because only edge averages are considered. Having these nonconforming spaces we can define a weak formulation as

$$\text{Find } \phi \in \mathcal{S} \quad : \quad (\phi_t, \psi) + \sum_{V \in \mathcal{V}} \int_V (\epsilon \nabla\phi \cdot \nabla\psi + \boldsymbol{\beta} \cdot \nabla\phi\,\psi)\, dV = (q, \psi) \text{ for all } \psi \in \mathcal{T}.$$

To obtain the semidiscretization we approximate the terms (ϕ_t, ψ) and (q, ψ) by (14). For constant velocity the remaining sum of integrals is evaluated exactly whereas a local approximation of the integrals $\int_V \boldsymbol{\beta}\nabla\phi\psi dV$ is applied for variable velocity field using the values $\beta_S \approx \beta(S)$.

The stiffness matrix $\boldsymbol{B}$ in (10) is assembled by the cell matrices

$$\begin{aligned}
\boldsymbol{B}_{V,i} &= \frac{|S_i|}{2}\Bigg\{\operatorname{cof}\left(\beta_{V,i}, \frac{2\epsilon}{|S_{i+1}|}\right)\begin{pmatrix} 4 & -2 & -2 \\ -2 & 1 & 1 \\ -2 & 1 & 1 \end{pmatrix} + \frac{2\epsilon}{|S_{i+1}|}\begin{pmatrix} 0 & 0 & 0 \\ 0 & 1 & -1 \\ 0 & -1 & 1 \end{pmatrix} \\
&\quad + \begin{pmatrix} 0 & -\beta_{S_{i+2},i} - \beta_{V,i} & \beta_{S_i,i} + \beta_{V,i} \\ \beta_{S_{i+2},i} + \beta_{V,i} & 0 & -\beta_{V,i} \\ -\beta_{S_i,i} - \beta_{V,i} & \beta_{V,i} & 0 \end{pmatrix}\Bigg\} \text{ for } V \in \mathcal{V} \text{ and } i = 1, 2\,, \\
B_S &= \boldsymbol{\beta}_S \cdot \boldsymbol{n}_S \text{ for } S \in \mathcal{S}_N\,.
\end{aligned}$$

The cell matrices $\boldsymbol{B}_{V,i}$ are connected to the cell vectors $\vec{u}_{V,i} := (u_V, u_{S_{i+2}}, u_{S_i})^T$ ignoring of rows and columns belonging to Dirichlet data u_S for $S \in \mathcal{S}_D$. The scalar B_S is associated with u_S for Neumann boundaries $S \in \mathcal{S}_N$. The function cof is defined by

$$\operatorname{cof}(\xi, \eta) = \begin{cases} \xi\left(\coth(\frac{\xi}{\eta}) - \frac{\eta}{\xi}\right)^{-1}, & \xi, \eta \neq 0 \\ |\xi|\,, & \eta = 0 \\ 3\eta\,, & \xi = 0 \end{cases}.$$

2.3 Time integration

The semidiscrete system (10) is a semi-explicit differential-algebraic system of index 1 since the submatrix $\boldsymbol{B}_{22}$ is regular [2].

The corresponding initial data $\vec{u}(0) = \vec{u}^0$ should be consistent in the sense that the algebraic equations are satisfied, i.e.

$$\boldsymbol{B}_{21}\vec{u}^0_{\mathcal{V}} + \boldsymbol{B}_{22}\vec{u}^0_{\mathcal{S}} = \vec{b}_2(0)\,.$$

Resolving the algebraic part of (10) for the variables $\vec{u}_{\mathcal{S}}$ and substituting into the differential part we get the underlying system

$$\boldsymbol{V}\frac{d}{dt}\vec{u}_{\mathcal{V}} + [\boldsymbol{B}/\boldsymbol{B}_{22}]\vec{u}_{\mathcal{V}} = \vec{b}_1 - \boldsymbol{B}_{12}\boldsymbol{B}_{22}^{-1}\vec{b}_2 \tag{15}$$

of ordinary differential equations where $[\boldsymbol{B}/\boldsymbol{B}_{22}] := \boldsymbol{B}_{11} - \boldsymbol{B}_{12}\boldsymbol{B}_{22}^{-1}\boldsymbol{B}_{21}$ denotes the Schur complement of $\boldsymbol{B}$. As a discrete analogue of the partial differential equation (1) this is a stiff system which describes the time behaviour of (10). Therefore it is reasonable to integrate (15) by implicit methods. Since the Schur complement should not be computed explicitly we make use of methods producing identical cell averages $\vec{u}_{\mathcal{V}}^n$ at time level n when applied to the semidiscretization (10) or the underlying system (15). At each time step it is necessary to solve one or more systems of linear equations having the form (for constant time steps Δt)

$$\boldsymbol{A}\vec{u} = \vec{f} \quad \text{with} \quad \boldsymbol{A} = \frac{\gamma}{\Delta t}\boldsymbol{M} + \boldsymbol{B}\,. \tag{16}$$

The parameter $\gamma > 0$ depends on the chosen method only. The vector $\vec{u}$ is either an approximation on the next time level or an increment.

Studying the quality of linear solvers for (16) it is adequate to restrict ourselves to the method of Gear (2-step backward differentiation formula) and the Crank-Nicolson scheme. These and other schemes including implicit Runge-Kutta methods are discussed in [5] with regard to this problem.

2.4 Convergence results

The following results are proved in [5]. Combining the asymptotic stability of the underlying system (15) which is uniformly in $h = \max\{|S|, S \in \mathcal{S}\}$ and the consistency of the semidiscretization with regard to the average values we obtain

Theorem 2.2 The cell orientated semidiscretization of the convection-diffusion problem (1, 2) is convergent of order 2 for quasi-uniform grids in the discrete l_2-norm $\|\vec{u}_{\mathcal{V}}\|^2 := \sum\limits_{V\in\mathcal{V}} |V| u_V^2$. This reduces to order 1 in the convection case $\epsilon = 0$ and also for an arbitrary rectangular grid.

With similar techniques as in the semidiscrete situation this theorem can be extended to the full discretization by using contractivity and convergence results for time integration methods.

Theorem 2.3 The cell orientated discretization is convergent in the grid parameter h with the order stated in Theorem 2.2 and of order 2 in Δt. For the method of Gear there is no restriction on the coupling of h and Δt.

2.5 Properties of the linear systems

First of all we ascertain that (16) is an illconditioned sparse linear system with a pattern of influence illustrated in fig 3. For the application of multigrid methods we analyse the definiteness of the stiffness matrix $\boldsymbol{B}$, the matrix $\boldsymbol{A}$ in (16) arising during time integration and the corresponding Schur complement. In the following we are assuming that $h_{min} := \min\{|S|, S \in \mathcal{S}\} \geq C_h h$ with a constant $C_h > 0$ independent of h.

Theorem 2.4 The stiffness matrix $\boldsymbol{B}$ is positive definite uniformly in h^2, i. e.

$$\vec{\Phi}^T \boldsymbol{B} \vec{\Phi} \geq \epsilon C h^2 \vec{\Phi}^T \vec{\Phi} \text{ for all } \vec{\Phi} \tag{17}$$

with a constant $C > 0$ independent of h.

Proof:

(i) We consider the quadratic form of $\boldsymbol{B}$ by assembling the cell matrices and estimating their local parts. Using the relations

$$\operatorname{cof}(\xi, \eta) \geq |\eta| \quad \text{and} \quad \boldsymbol{\beta}_S \cdot \boldsymbol{n}_S \geq 0 \text{ for } S \in \partial \mathcal{S}_N$$

we obtain for a parameter $\alpha \in (0, 3]$

$$\begin{aligned}
\vec{\Phi}^T \boldsymbol{B} \vec{\Phi} &= \sum_{V \in \mathcal{V}} \sum_{i=1}^{2} \vec{\Phi}_{V,i}^T \boldsymbol{B}_{V,i} \vec{\Phi}_{V,i} + \sum_{S \in \partial \mathcal{S}_N} \boldsymbol{B}_S \Phi_S^2 \\
&\geq \epsilon \sum_{V \in \mathcal{V}} \sum_{i=1}^{2} \frac{|S_i|}{|S_{i+1}|} \vec{\Phi}_{V,i}^T \left\{ 3 \begin{pmatrix} 4 & -2 & -2 \\ -2 & 1 & 1 \\ -2 & 1 & 1 \end{pmatrix} + \begin{pmatrix} 0 & 0 & 0 \\ 0 & 1 & -1 \\ 0 & -1 & 1 \end{pmatrix} \right\} \vec{\Phi}_{V,i} \\
&\geq \epsilon C_h \sum_{V \in \mathcal{V}} \sum_{i=1}^{2} \vec{\Phi}_{V,i}^T \boldsymbol{K}_{V,i}(\alpha) \vec{\Phi}_{V,i} \\
&=: \epsilon C_h \vec{\Phi}^T \boldsymbol{K}(\alpha) \vec{\Phi}
\end{aligned}$$

with

$$\boldsymbol{K}_{V,i}(\alpha) := \alpha \begin{pmatrix} 4 & -2 & -2 \\ -2 & 1 & 1 \\ -2 & 1 & 1 \end{pmatrix} + \begin{pmatrix} 0 & 0 & 0 \\ 0 & 1 & -1 \\ 0 & -1 & 1 \end{pmatrix}. \tag{18}$$

In contrast to $\boldsymbol{B}$ the matrix $\boldsymbol{K}(\alpha)$ is symmetric and independent of $\boldsymbol{\beta}$. The elimination of the Dirichlet data is formally done by setting $\Phi_S := 0$, $S \in \partial \mathcal{S}_D$ in the cell vectors $\vec{\Phi}_{V,i}$.

(ii) Since $\boldsymbol{K}_{11}$ is diagonal the Schur complement $[\boldsymbol{K}/\boldsymbol{K}_{11}](\alpha)$ can be computed in terms of the cell matrices $\boldsymbol{K}_{V,i}(\alpha)$ locally (static condensation). Choosing $\alpha = 2$ $[\boldsymbol{K}/\boldsymbol{K}_{11}](2)$ can be interpreted as a finite-difference discretization of $-\Delta u = 0$ with a crossed 5-point-stencil shown in fig 4. Thereby it is well-known that

$$\vec{\Phi}_{\mathcal{S}}^T [\boldsymbol{K}/\boldsymbol{K}_{11}](2) \vec{\Phi}_{\mathcal{S}} \geq C_1 h^2 \vec{\Phi}_{\mathcal{S}}^T \vec{\Phi}_{\mathcal{S}}\,. \tag{19}$$

By setting $\alpha = 1$ the matrix $\boldsymbol{K}_{22}(1)$ is also diagonal. This leads to $[\boldsymbol{K}/\boldsymbol{K}_{22}](1)$ as the standard 5-point-stencil of the Laplacian (see fig 4). Therefore we have

$$\vec{\Phi}_{\mathcal{V}}^T [\boldsymbol{K}/\boldsymbol{K}_{22}](1) \vec{\Phi}_{\mathcal{V}} \geq C_2 h^2 \vec{\Phi}_{\mathcal{V}}^T \vec{\Phi}_{\mathcal{V}}\,. \tag{20}$$

The constants $C_1, C_2 > 0$ are independent of h.

(iii) Splitting the quadratic form of $\boldsymbol{K} = \boldsymbol{K}(\alpha)$ into two parts using the Schur complements we have for arbitrary $\alpha \in (0, 3]$

$$\vec{\Phi}^T \boldsymbol{K} \vec{\Phi} = \vec{\Phi}_{\mathcal{V}}^T [\boldsymbol{K}/\boldsymbol{K}_{22}] \vec{\Phi}_{\mathcal{V}} + \tilde{\vec{\Phi}}_{\mathcal{S}}^T \boldsymbol{K}_{22} \tilde{\vec{\Phi}}_{\mathcal{S}} \geq \vec{\Phi}_{\mathcal{V}}^T [\boldsymbol{K}/\boldsymbol{K}_{22}] \vec{\Phi}_{\mathcal{V}}$$

with

$$\tilde{\vec{\Phi}}_{\mathcal{S}} = \vec{\Phi}_{\mathcal{S}} + \boldsymbol{K}_{22}^{-1} \boldsymbol{K}_{12} \vec{\Phi}_{\mathcal{V}}$$

and

$$\vec{\Phi}^T \boldsymbol{K} \vec{\Phi} = \vec{\Phi}_{\mathcal{S}}^T [\boldsymbol{K}/\boldsymbol{K}_{11}] \vec{\Phi}_{\mathcal{S}} + \tilde{\vec{\Phi}}_{\mathcal{V}}^T \boldsymbol{K}_{11} \tilde{\vec{\Phi}}_{\mathcal{V}} \geq \vec{\Phi}_{\mathcal{S}}^T [\boldsymbol{K}/\boldsymbol{K}_{11}] \vec{\Phi}_{\mathcal{S}}$$

with

$$\tilde{\vec{\Phi}}_{\mathcal{V}} = \vec{\Phi}_{\mathcal{V}} + \boldsymbol{K}_{11}^{-1} \boldsymbol{K}_{21} \vec{\Phi}_{\mathcal{S}} \,.$$

Combining these results with equations (18), (19) and (20) we obtain finally

$$\begin{aligned} \vec{\Phi}^T \boldsymbol{B} \vec{\Phi} &\geq \epsilon C_h h^2 \max\{C_1 \vec{\Phi}_{\mathcal{S}}^T \vec{\Phi}_{\mathcal{S}}, C_2 \vec{\Phi}_{\mathcal{V}}^T \vec{\Phi}_{\mathcal{V}}\} \\ &\geq \epsilon C_h h^2 \min\{C_1, C_2\} \frac{1}{2} \left(\vec{\Phi}_{\mathcal{S}}^T \vec{\Phi}_{\mathcal{S}} + \vec{\Phi}_{\mathcal{V}}^T \vec{\Phi}_{\mathcal{V}} \} \right) \\ &= \epsilon C h^2 \vec{\Phi}^T \vec{\Phi} \quad \text{with} \quad C := \frac{1}{2} C_h \min\{C_1, C_2\} \,. \end{aligned}$$

□

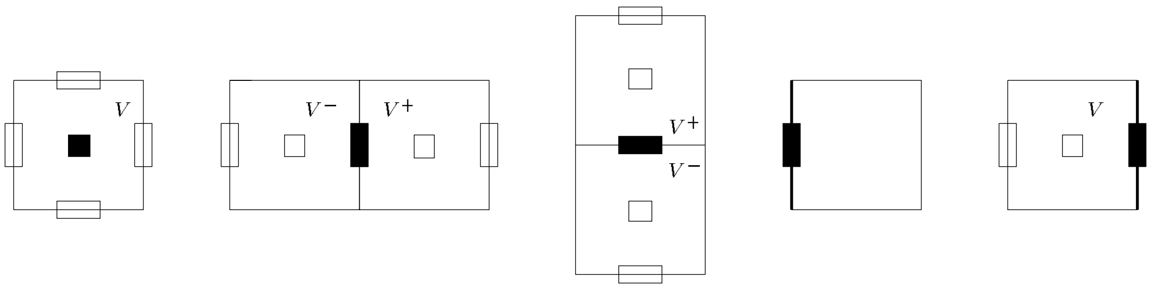

Figure 3: Pattern of influence

Corollary 2.5 The matrix $\boldsymbol{A}$ of (16) and its Schur complement $[\boldsymbol{A}/\boldsymbol{A}_{22}]$ are positive definite uniformly in h^2, i. e.

$$\vec{\Phi}^T \boldsymbol{A} \vec{\Phi} \geq \epsilon \, C h^2 \vec{\Phi}^T \vec{\Phi} \text{ for all } \vec{\Phi} \tag{21}$$

and

$$\vec{\Phi}_{\mathcal{V}}^T [\boldsymbol{A}/\boldsymbol{A}_{22}] \vec{\Phi}_{\mathcal{V}} \geq \left(\epsilon \, C + \frac{\gamma}{\Delta t} C_h^2 \right) h^2 \vec{\Phi}_{\mathcal{V}}^T \vec{\Phi}_{\mathcal{V}} \text{ for all } \vec{\Phi}_{\mathcal{V}}$$

where $C > 0$ is the constant from (17).

Proof: The definition of $\boldsymbol{M}$ in (10) yields

$$\vec{\Phi}^T \boldsymbol{M} \vec{\Phi} = \vec{\Phi}_{\mathcal{V}}^T \boldsymbol{V} \vec{\Phi}_{\mathcal{V}} \geq \min_{V \in \mathcal{V}} \{|V|\} \vec{\Phi}_{\mathcal{V}}^T \vec{\Phi}_{\mathcal{V}} \geq C_h^2 h^2 \vec{\Phi}_{\mathcal{V}}^T \vec{\Phi}_{\mathcal{V}} \geq 0. \tag{22}$$

In combination with (16) and (17) this gives (21) directly.

The connection between the Schur complement $[\boldsymbol{B}/\boldsymbol{B}_{22}]$ and $\boldsymbol{B}$ is established by

$$\vec{\Phi}^T \boldsymbol{B} \vec{\Phi} = \vec{\Phi}_{\mathcal{V}}^T [\boldsymbol{B}/\boldsymbol{B}_{22}] \vec{\Phi}_{\mathcal{V}} \quad \text{with} \quad \vec{\Phi} := \begin{pmatrix} \boldsymbol{I} \\ -\boldsymbol{B}_{22}^{-1} \boldsymbol{B}_{21} \end{pmatrix} \vec{\Phi}_{\mathcal{V}} \tag{23}$$

for arbitrary $\vec{\Phi}_{\mathcal{V}}$.

From $[\boldsymbol{A}/\boldsymbol{A}_{22}] = \frac{\gamma}{\Delta t} \boldsymbol{V} + [\boldsymbol{B}/\boldsymbol{B}_{22}]$, (17), (22) and (23) we have the estimation

$$\begin{aligned} \vec{\Phi}_{\mathcal{V}}^T [\boldsymbol{A}/\boldsymbol{A}_{22}] \vec{\Phi}_{\mathcal{V}} = \frac{\gamma}{\Delta t} \vec{\Phi}_{\mathcal{V}}^T \boldsymbol{V} \vec{\Phi}_{\mathcal{V}} + \vec{\Phi}^T \boldsymbol{B} \vec{\Phi} &\geq \frac{\gamma}{\Delta t} C_h^2 h^2 \vec{\Phi}_{\mathcal{V}}^T \vec{\Phi}_{\mathcal{V}} + \epsilon C h^2 \vec{\Phi}^T \vec{\Phi} \\ &\geq \left(\epsilon C + \frac{\gamma}{\Delta t} C_h^2 \right) h^2 \vec{\Phi}_{\mathcal{V}}^T \vec{\Phi}_{\mathcal{V}}. \end{aligned}$$

$\square$

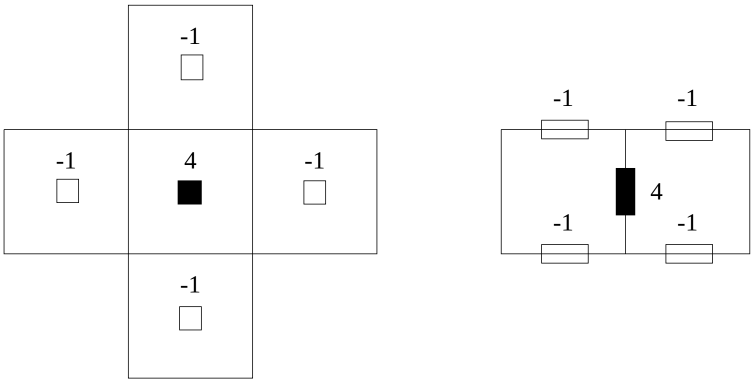

Figure 4: 5-point stencil and crossed 5-point stencil

3 Multigrid iteration

3.1 Basic multigrid algorithm

For solving the linear system (16) by a multigrid method we consider the discretization matrices

$$\boldsymbol{A}^0, \boldsymbol{A}^1, \dots \boldsymbol{A}^{l_{max}} = \boldsymbol{A} \quad \text{with} \quad \boldsymbol{A}^l \in \mathbb{R}^{N_l \times N_l}$$

on a sequence of nested grids

$$\mathcal{G}_0 \subset \mathcal{G}_1 \subset \dots \subset \mathcal{G}_{l_{max}}$$

Let $\boldsymbol{s}^l : \mathbb{R}^{N_l} \to \mathbb{R}^{N_l}$ be a smoothing iteration, $\boldsymbol{p}^l : \mathbb{R}^{N_{l-1}} \to \mathbb{R}^{N_l}$ a prolongation and $\boldsymbol{r}^l : \mathbb{R}^{N_l} \to \mathbb{R}^{N_{l-1}}$ a restriction operator for $l = 1, \dots, l_{max}$. The (multiplicative) multigrid method then reads (see [1, 3, 13])

Algorithm 3.1

$\mathbf{MGM}(l, \vec{u}, \vec{f})$

if $\quad (l = 0)$

$\vec{u} \quad := \quad (\boldsymbol{A}^0)^{-1}\vec{f}$ *(exact solution on coarsest grid)*

else

$\vec{u} \quad := \quad \boldsymbol{s}^l(\vec{u}, \vec{f}; \nu_1)$ *(presmoothing)*

$\vec{d} \quad := \quad \boldsymbol{r}^l(\boldsymbol{A}^l\vec{u} - \vec{f})$ *(restriction of defect)*

$\vec{v} \quad := \quad 0$

for $\quad j = 1, \ldots, \mu \quad$ do $\mathbf{MGM}(l-1, \vec{v}, \vec{d})$

$\vec{u} \quad := \quad \vec{u} - \boldsymbol{p}^l\vec{v}$ *(coarse grid correction)*

$\vec{u} \quad := \quad \boldsymbol{s}^l(\vec{u}, \vec{f}; \nu_2)$ *(postsmoothing)*

endif

For the choice of $\mu = 1$ we get the V-cycle and for $\mu = 2$ the W-cycle. As mentioned in the introduction the Gauss-Seidel and the ILU iteration [4, 6] are fast solvers in the convection dominated case in combination with a numbering in direction of the velocity field. We are using these methods as smoothing iterations in our computations. For the solution on the coarsest grid we are making use of the GMRES method [10, 14]. The number of iterations in pre- and postsmoothing are denoted by ν_1 and ν_2, respectively.

3.2 Restriction and prolongation

For the description of restriction and prolongation operators we assume that a cell V belonging to $\mathcal{G}_{l-1}$ consists of four adjacent fine grid cells $\tilde{V}_k$ on level l as shown in fig 5. The two interpretations of our discretization lead to different constructions of these operators. The index l is neglected when the meaning is obvious.

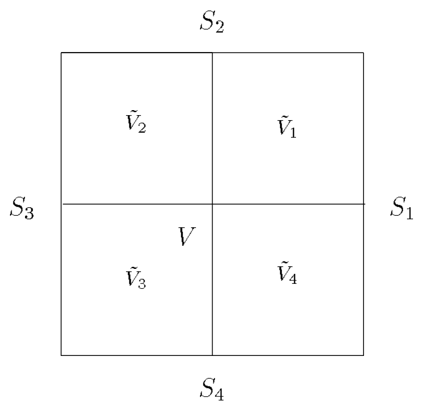

Figure 5: local notations

3.2.1 Finite volume approach

The underlying system (15) of ordinary differential equations motivates to understand the differential part of the semidiscrete system (10) as finite volume equations and the algebraic part as constraints. Transferring this point of view to the linear system (16) we consider first of all the Schur complement system

$$[\boldsymbol{A}/\boldsymbol{A}_{22}]\vec{u}_{\mathcal{V}} = \vec{f}_1 - \boldsymbol{A}_{12}\boldsymbol{A}_{22}{}^{-1}\vec{f}_2 = \vec{f}_{\text{Schur}} \tag{24}$$

which determines the cell averages $\vec{u}_{\mathcal{V}}$ independently of the edge averages $\vec{u}_{\mathcal{S}}$. Thus, we have to derive a restriction and prolongation for the parts corresponding to cells.

The defect vector for this Schur complement system is given by $\vec{d}_{\mathcal{V}} = [\boldsymbol{A}/\boldsymbol{A}_{22}]\vec{u}_{\mathcal{V}} - \vec{f}_{\text{Schur}}$. Its components d_V should be approximations to the integral of a defect function $\tilde{d}(\boldsymbol{x})$, i.e.

$$d_V \approx \int_V \tilde{d}(\boldsymbol{x})d\boldsymbol{x} \tag{25}$$

which is motivated by the finite volume approach described in section 2.1.

This defines a restriction $\boldsymbol{r}^l_{\mathcal{V}}$ by means of

$$(\boldsymbol{r}^l_{\mathcal{V}}\vec{d}^l_{\mathcal{V}})_V := \sum_{i=1}^{4} d^l_{\tilde{V}_i} \approx \sum_{i=1}^{4}\int_{\tilde{V}_i}\tilde{d}(\boldsymbol{x})d\boldsymbol{x} = \int_V \tilde{d}(\boldsymbol{x})d\boldsymbol{x} \approx d^{l-1}_V \text{ for all } V \in \mathcal{V}. \tag{26}$$

With respect to the scalar products $\vec{d}^T_{\mathcal{V}}\boldsymbol{V}^{-1}\vec{d}_{\mathcal{V}}$ for defect vectors and $\vec{u}^T_{\mathcal{V}}\boldsymbol{V}\vec{u}_{\mathcal{V}}$ for cell averages the corresponding prolongation $\boldsymbol{p}^l_{\mathcal{V}}$ simply reads

$$\boldsymbol{p}^l_{\mathcal{V}} = (\boldsymbol{r}^l_{\mathcal{V}})^T. \tag{27}$$

The resulting multigrid algorithm is not really efficient since the Schur complement $[\boldsymbol{A}/\boldsymbol{A}_{22}]$ should not be computed explicitly. Hence we have to extend the grid transfer operators including the edge components to get a comparable multigrid method for the whole system.

The matrix $\boldsymbol{A}$ can be decoupled by the block decomposition

$$\boldsymbol{A} = \begin{pmatrix} \boldsymbol{I} & \boldsymbol{A}_{12}\boldsymbol{A}_{22}^{-1} \\ \boldsymbol{0} & \boldsymbol{I} \end{pmatrix}\begin{pmatrix} [\boldsymbol{A}/\boldsymbol{A}_{22}] & \boldsymbol{0} \\ \boldsymbol{0} & \boldsymbol{A}_{22} \end{pmatrix}\begin{pmatrix} \boldsymbol{I} & \boldsymbol{0} \\ \boldsymbol{A}_{22}^{-1}\boldsymbol{A}_{21} & \boldsymbol{I} \end{pmatrix} = (\boldsymbol{I}+\boldsymbol{U})\hat{\boldsymbol{A}}(\boldsymbol{I}+\boldsymbol{L}) \tag{28}$$

where the back transformations are given by the identities $(\boldsymbol{I}+\boldsymbol{U})(\boldsymbol{I}-\boldsymbol{U}) = \boldsymbol{I}$ and $(\boldsymbol{I}+\boldsymbol{L})(\boldsymbol{I}-\boldsymbol{L}) = \boldsymbol{I}$. Using this we are able to define a decoupled system by $\hat{\boldsymbol{A}}\hat{\boldsymbol{u}} = \hat{\boldsymbol{f}}$ with $\hat{\boldsymbol{u}} = (\boldsymbol{I}+\boldsymbol{L})\boldsymbol{u}$ and $\hat{\boldsymbol{f}} = (\boldsymbol{I}-\boldsymbol{U})\boldsymbol{f}$.

For this system the restriction and the prolongation should also be decoupled, i.e.

$$\hat{\boldsymbol{r}}^l := \begin{pmatrix} \boldsymbol{r}^l_{\mathcal{V}} & \boldsymbol{0} \\ \boldsymbol{0} & \boldsymbol{r}^l_{\mathcal{S}} \end{pmatrix}, \quad \hat{\boldsymbol{p}}^l := \begin{pmatrix} \boldsymbol{p}^l_{\mathcal{V}} & \boldsymbol{0} \\ \boldsymbol{0} & \boldsymbol{p}^l_{\mathcal{S}} \end{pmatrix} \tag{29}$$

with $\boldsymbol{r}_{\mathcal{V}}^l$ and $\boldsymbol{p}_{\mathcal{V}}^l$ from (26, 27) and analogously

$$(\boldsymbol{r}_{\mathcal{S}}^l \vec{d}_{\mathcal{S}}^l)_S := \sum_{i=1}^{2} d_{\tilde{S}_i}^l, \quad \boldsymbol{p}_{\mathcal{S}}^l = (\boldsymbol{r}_{\mathcal{S}}^l)^T \text{ for all } S \in \mathcal{S} \tag{30}$$

where $\tilde{S}_1, \tilde{S}_2$ are the fine grid parts of S.

Assuming that the defect vector transforms like the right hand side and the correction vector like a solution vector the corresponding transfer operators of the original system are

$$\boldsymbol{r}^l := (\boldsymbol{I} + \boldsymbol{U}^{l-1})\hat{\boldsymbol{r}}^l(\boldsymbol{I} - \boldsymbol{U}^l), \tag{31}$$

$$\boldsymbol{p}^l := (\boldsymbol{I} - \boldsymbol{L}^l)\hat{\boldsymbol{p}}^l(\boldsymbol{I} + \boldsymbol{L}^{l-1}). \tag{32}$$

Theorem 3.2 Under the assumption of exact solution on the coarse grid the defect corrections for the cell variables according to the Schur complement system (24) and the original system (16) are identical.

Proof: The correction vector belonging to (16) is defined by

$$\Delta\vec{u}^l = \boldsymbol{p}^l(\boldsymbol{A}^{l-1})^{-1}\boldsymbol{r}^l\left(\boldsymbol{A}\vec{u}^l - \vec{f}^l\right)$$

and for the Schur complement system by

$$\Delta\vec{u}^l{}_{\text{Schur}} = \boldsymbol{p}_{\mathcal{V}}^l\left([\boldsymbol{A}/\boldsymbol{A}_{22}]^{l-1}\right)^{-1}\boldsymbol{r}_{\mathcal{V}}^l\left([\boldsymbol{A}/\boldsymbol{A}_{22}]^l\vec{u}_{\mathcal{V}}^l - \vec{f}^l{}_{\text{Schur}}\right)$$

with exact solution on the coarse level $l-1$. Hence we have to show that

$$\left(\Delta\vec{u}^l\right)_{\mathcal{V}} = \Delta\vec{u}^l{}_{\text{Schur}}. \tag{33}$$

Using the definitions (31, 32) for the restriction and the prolongation, the factorization (28) and the block diagonal structure of $\hat{\boldsymbol{p}}^l$, $\hat{\boldsymbol{r}}^l$ and $\hat{\boldsymbol{A}}^{l-1}$ we get

$$\begin{aligned}
\Delta\vec{u}^l &= (\boldsymbol{I} - \boldsymbol{L}^l)\hat{\boldsymbol{p}}^l(\boldsymbol{I} + \boldsymbol{L}^{l-1})\left(\boldsymbol{A}^{l-1}\right)^{-1}(\boldsymbol{I} + \boldsymbol{U}^{l-1})\hat{\boldsymbol{r}}^l(\boldsymbol{I} - \boldsymbol{U}^l)\left(\boldsymbol{A}^l\vec{u}^l - \vec{f}^l\right) \\
&= (\boldsymbol{I} - \boldsymbol{L}^l)\hat{\boldsymbol{p}}^l\left(\hat{\boldsymbol{A}}^{l-1}\right)^{-1}\hat{\boldsymbol{r}}^l\left(\hat{\boldsymbol{A}}^l(\boldsymbol{I} + \boldsymbol{L}^l)\vec{u}^l - (\boldsymbol{I} - \boldsymbol{U}^l)\vec{f}^l\right) \\
&= (\boldsymbol{I} - \boldsymbol{L}^l)\begin{pmatrix} \hat{\boldsymbol{p}}_{\mathcal{V}}^l\left([\boldsymbol{A}/\boldsymbol{A}_{22}]^{l-1}\right)^{-1}\boldsymbol{r}_{\mathcal{V}}^l & \boldsymbol{0} \\ \boldsymbol{0} & \hat{\boldsymbol{p}}_{\mathcal{S}}^l(\boldsymbol{A}_{22}^{l-1})^{-1}\hat{\boldsymbol{r}}_{\mathcal{S}}^l \end{pmatrix}\begin{pmatrix} [\boldsymbol{A}/\boldsymbol{A}_{22}]^l\vec{u}_{\mathcal{V}}^l - \vec{f}^l{}_{\text{Schur}} \\ \boldsymbol{A}_{21}^l\vec{u}_{\mathcal{V}}^l + \boldsymbol{A}_{22}^l\vec{u}_{\mathcal{S}}^l - \vec{f}_2^l \end{pmatrix}.
\end{aligned}$$

Evaluating the cell part of this product the assertion (33) follows directly. □

For the implementation of the operators (29) it is important that a system with the matrix $\boldsymbol{A}_{22}$ can be solved at low costs.

Remark 3.3 The matrix $\boldsymbol{A}_{22} = \boldsymbol{B}_{22}$ of *(16)* is strictly diagonal dominant for $\epsilon > 0$ and reduces to triangular form for $\epsilon = 0$ with a numbering in convection direction. For that reason the Gauss-Seidel method is a fast solver for systems involving this matrix. This is also true for the ILU iteration.

3.2.2 Petrov-Galerkin approach

For finite element methods the prolongation and restriction operator are naturally defined in terms of the nodal functions using the corresponding function spaces [3].

For a conforming method with nested finite element spaces $\mathcal{S}^0 \subset \mathcal{S}^1 \subset \cdots \subset \mathcal{S}^{l_{max}}$ and a nodal basis $\mathcal{S}^l = \mathrm{span}\{\Phi^{l,i}, i = 1, \ldots, N_l\}$ we can express the nodal functions on level $l-1$ by

$$\Phi^{l-1,j}(\boldsymbol{x}) = \sum_{i=1}^{N_l} \Phi^{l-1,j}(i)\Phi^{l,i}(\boldsymbol{x}) \, , j = 1, \ldots, N_{l-1}$$

where $\Phi(i)$ denotes the nodal value of Φ for the index i. Hence we have the identity

$$u^{l-1}(\boldsymbol{x}) = \sum_{j=1}^{N_{l-1}} u_j^{l-1}\Phi^{l-1,j}(\boldsymbol{x}) = \sum_{i=1}^{N_l}\sum_{j=1}^{N_{l-1}} \Phi^{l-1,j}(i)u_j^{l-1}\Phi^{l-1,j}(\boldsymbol{x}).$$

The canonical prolongation $\tilde{p}^l$ on the ansatz spaces is defined by the inclusion

$$\mathcal{S}^l \ni \tilde{p}^l u^{l-1} = u^{l-1} = \sum_{i=1}^{N_l}\sum_{j=1}^{N_{l-1}} \Phi^{l-1,j}(i)u_j^{l-1}\Phi^{l,i} \in \mathcal{S}^{l-1}$$

with the prolongation matrix given as

$$(\boldsymbol{p}^l)_{ij} = \Phi^{l-1,j}(i) \quad \text{for} \quad i = 1, \ldots, N_l, \quad j = 1, \ldots, N_{l-1}.$$

The corresponding restriction matrix $\boldsymbol{r}^l$ for the residuals tested by the nodal functions is

$$\boldsymbol{r}^l = (\boldsymbol{p}^l)^T.$$

Considering Petrov-Galerkin methods the prolongation is connected to the trial spaces $\mathcal{S}^l$ and the restriction to the test spaces $\mathcal{T}^l$. Therefore we have

$$(\boldsymbol{p}^l)_{ij} = \Phi^{l-1,j}(i), \quad (\boldsymbol{r}^l)_{ji} = \Psi^{l-1,j}(i) \quad \text{for} \quad i = 1, \ldots, N_l, \quad j = 1, \ldots, N_{l-1}.$$

In our case the nodal values are the averages (5) indexed by $V \in \mathcal{V}$ and $S \in \mathcal{S}$ instead of i. For the one-dimensional problem the evaluation is evident. In two dimensions we have to deal with nonconforming nodal functions. Due to the discontinuity at the boundary D of $\mathrm{supp}(\Phi^{l-1,j})$ and $\mathrm{supp}(\Psi^{l-1,j})$. We define the edge averages for $\mathcal{S} \subset D$ to be zero as it would be in the conforming case:

$$\Phi^{l-1,j}(S) := \begin{cases} \frac{1}{2}\Phi^{l-1,j}{}_{|D}(S) & \text{for} \quad S \in \mathcal{S} \setminus \partial\mathcal{S} \\ \Phi^{l-1,j}{}_{|D}(S) & \text{for} \quad S \in \partial\mathcal{S} \end{cases}$$

and for the restriction, analogously.

Fig 6 illustrates the prolongation and restrictions for the limit cases of the diffusion and the convection problem in form of collection stencils for $\boldsymbol{r}^l$ and distribution stencils for $\boldsymbol{p}^l$.

$$
\left]\begin{array}{ccccc}
 & 0 & & 0 & \\
0 & 1 & 3/2 & 1 & 0 \\
 & 3/2 & \blacksquare & 3/2 & \\
0 & 1 & 3/2 & 1 & 0 \\
 & 0 & & 0 &
\end{array}\right[
\qquad
\left]\begin{array}{ccccccccc}
 & 0 & & 0 & & 0 & & 0 & \\
0 & -1/4 & -1/4 & 1/4 & 1 & 1/4 & -1/4 & -1/4 & 0 \\
 & -1/4 & & 1/4 & \blacksquare & 1/4 & & -1/4 & \\
0 & -1/4 & -1/4 & 1/4 & 1 & 1/4 & -1/4 & -1/4 & 0 \\
 & 0 & & 0 & & 0 & & 0 &
\end{array}\right[
$$

$$
\left]\begin{array}{ccccc}
 & 0 & & 0 & \\
0 & 1 & 3/2 & 2 & 0 \\
 & 1/2 & \blacksquare & 3/2 & \\
0 & 0 & 1/2 & 1 & 0 \\
 & 0 & & 0 &
\end{array}\right[
\qquad
\left]\begin{array}{ccccccccc}
 & 0 & & 0 & & 0 & & 0 & \\
0 & 0 & 0 & 0 & 1 & 1/2 & 0 & -1/2 & 0 \\
 & 0 & & 0 & \blacksquare & 1/2 & & -1/2 & \\
0 & 0 & 0 & 0 & 1 & 1/2 & 0 & -1/2 & 0 \\
 & 0 & & 0 & & 0 & & 0 &
\end{array}\right[
$$

$$
\left[\begin{array}{ccccc}
 & 0 & & 0 & \\
0 & 1 & 1/2 & 0 & 0 \\
 & 3/2 & \blacksquare & 1/2 & \\
0 & 2 & 3/2 & 1 & 0 \\
 & 0 & & 0 &
\end{array}\right]
\qquad
\left[\begin{array}{ccccccccc}
 & 0 & & 0 & & 0 & & 0 & \\
0 & -1/2 & 0 & 1/2 & 1 & 0 & 0 & 0 & 0 \\
 & -1/2 & & 1/2 & \blacksquare & 0 & & 0 & \\
0 & -1/2 & 0 & 1/2 & 1 & 0 & 0 & 0 & 0 \\
 & 0 & & 0 & & 0 & & 0 &
\end{array}\right]
$$

Figure 6: Prolongation and restriction

4 Numerical results

For our numerical computations we consider four test problems [5, 9, 12] for the linear convection-diffusion equation (1, 2).

Problem 4.1

$$Lu = 0 \quad \text{in } \Omega = (0,1) \times (0,1)$$

with $\boldsymbol{\beta} = (\cos\alpha, \sin\alpha)^T$ and $u(x,y) = x^2 + y^2$ on Γ. The angle α is varying in multiples of $15°$.

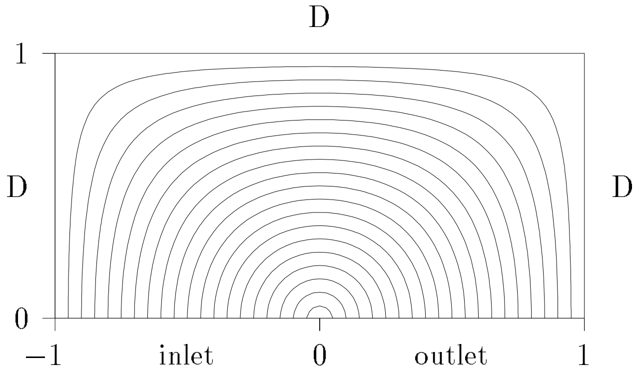

Figure 7: Streamlines and boundary conditions for problem 4.2

Problem 4.2

$$Lu = 0 \quad \text{in } \Omega = (-1,1) \times (0,1)$$

with $\boldsymbol{\beta} = (-\psi_y, \psi_x)^T$ given by the stream function $\psi = (1-x^2)(1-y^2)$ and

$$\begin{aligned} u(x,y) &= \begin{cases} 1 + \tanh(10[2x+1]) & \text{on } \Gamma_{\text{inlet}} := \{(x,y) \in \Gamma : -1 \le x \le 0, y = 0)\}\,, \\ 0 & \text{on } \Gamma_D \setminus \{\Gamma_{\text{inlet}} \cup \Gamma_N\}\,, \end{cases} \\ \partial u_n(x,y) &= 0 \quad \text{on } \Gamma_N := \{(x,y) \in \Gamma : 0 \le x \le 1, y = 0)\}\,. \end{aligned}$$

Problem 4.3

$$u_t - \Delta u = 0 \quad \text{in } \Omega = (0,1) \times (0,1) \quad \text{with}$$

$$\begin{aligned} u(x,y) &= 0 \quad \text{on } \Gamma_D := \{(x,y) \in \Gamma : x = 0 \text{ or } y = 0)\} \\ \partial u_n(x,y) &= 0 \quad \text{on } \Gamma_N := \Gamma \setminus \Gamma_D. \end{aligned}$$

The initial condition is taken from the exact solution

$$u(\boldsymbol{x},t) = \sin(\frac{\pi}{2}x)\sin(\frac{\pi}{2}y)\exp(-\frac{\pi^2}{2}t) + \sin(\frac{3\pi}{2}x)\sin(\frac{3\pi}{2}y)\exp(\frac{-9\pi^2}{2}t). \quad (34)$$

Problem 4.4 (rotating hump)

$$u_t + \boldsymbol{\beta} \cdot \boldsymbol{\nabla} u = 0 \quad \text{in } \Omega = (-1,1) \times (-1,1)$$

with $\boldsymbol{\beta} = (-\psi_y, \psi_x)^T$, $\psi = \frac{x^2+y^2}{2}$ and

$$\begin{aligned} u(\boldsymbol{x},0) &= \begin{cases} \frac{1}{2}\left(1 + \cos(\frac{5}{2}\pi r)\right) & \text{in } r = \|\boldsymbol{x} - \boldsymbol{x}_0\|_2 \le \frac{2}{5}\,, \\ 0 & \text{else}\,, \end{cases} \\ u(\boldsymbol{x},t) &= 0 \quad \text{on } \Gamma\,. \end{aligned}$$

First of all we have to illustrate the quality of the cell-orientated discretization. This is influenced by the approximation in space mainly. Therefore it is convenient to consider the steady problem 4.2. Fig 8 shows the results on a 40×40 grid and various values of ϵ. The isolines of the computed solution depicted on the left are indicating that there is no artifical crosswind diffusion. And on the right hand side the good coincidence between the nodal values of the approximation and the exact solution can be observed [11].

As a smoother we consider the Gauss-Seidel and ILU iteration which are exact solvers in the convection case with a numbering in the direction of the velocity. This governs the excellent behaviour of the multigrid method in convection dominated cases. On the other hand the Gauss-Seidel method (GS) leads to low efficiency for diffusion dominated problems. This difficulty can be weakened by choosing a relaxation factor greater than 1, e.g. $\omega = 1.25$ in the SOR method. Unfortunately we achieve a breakdown in the convection dominated case. Another alternative for the diffusion equation is the use of alternating line Gauss-Seidel iterations which is not suitable for a numeration in the

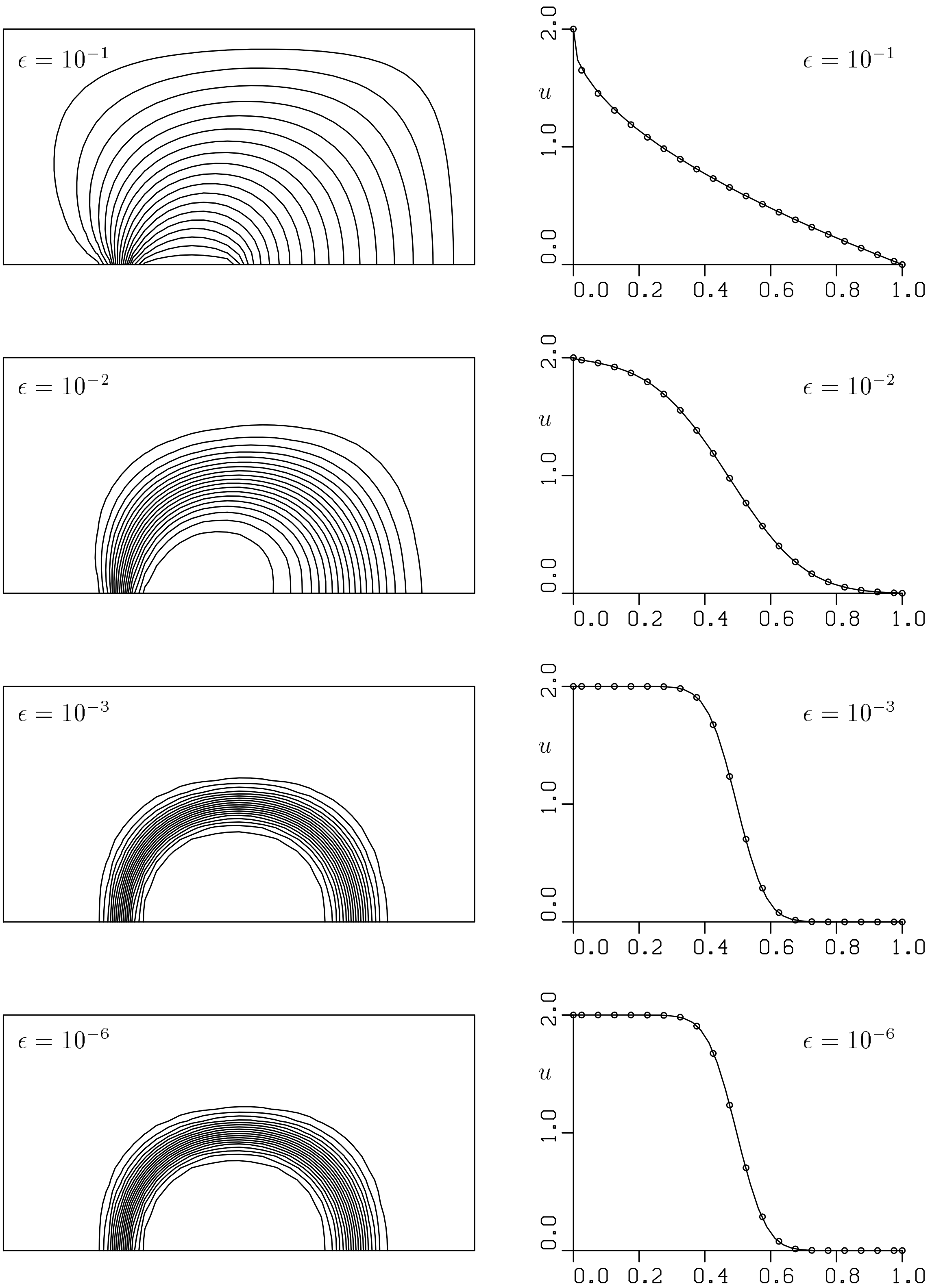

Figure 8: The quality of the cell orientated discretization

direction of the velocity [7].

The averaged reduction factor is defined by

$$\varrho_M := \left(\frac{\|r_\kappa\|_2}{\|r_0\|_2}\right)^{\frac{1}{\kappa}} \quad \text{with } \kappa = \text{number of multigrid cycles}.$$

We illustrate the behaviour of different smoothers for problem 4.1 with various parameters on a 64×64 grid with 12416 unknowns. Table 10 shows the reduction factor ϱ_M for the finite volume transfer operators and table 9 for the operators corresponding to the Petrov-Galerkin interpretation. For all computations we set the number of pre- and postsmoothing iterations to $\nu_1 = \nu_2 = 2$.

smoothing iteration	$\varepsilon \setminus \alpha$	$0°$	$15°$	$30°$	$45°$	$60°$	$75°$	$90°$	$135°$	$-45°$
ILU	1	.268	.272	.272	.272	.272	.272	.268	.258	.258
	0.1	.215	.215	.221	.223	.221	.215	.215	.225	.225
	0.01	.087	.097	.085	.079	.085	.097	.087	.096	.097
	0.001	.028	.010	.005	.003	.005	.010	.028	.022	.022
GS	1	.911	.908	.906	.905	.906	.908	.911	.905	.905
	0.1	.870	.855	.845	.840	.845	.855	.869	.842	.842
	0.01	.369	.352	.324	.310	.324	.352	.369	.345	.345
	0.001	.087	.047	.025	.015	.025	.047	.087	.061	.061
SOR ($\omega = 1.25$)	1	.720	.702	.704	.701	.704	.702	.720	.700	.700
	0.1	.630	.610	.594	.586	.594	.610	.630	.556	.556
	0.01	.260	.193	.170	.162	.170	.193	.260	.161	.161

Table 9: Finite volume restriction and prolongation

Comparing these two tables we can see that the convergence for restriction and prolongation of the finite volume type is much better than in the Petrov-Galerkin case. As expected the reduction factor is very good for ϵ small. Anyway we have to mention that the multigrid method does not converge for the SOR method and $\epsilon = 0.001$ as well as in the Petrov-Galerkin case for the Gauss-Seidel iteration and $\epsilon = 1$. The crucial point for the choice of the smoothing iteration is the reduction factor for the diffusion dominated case ($\epsilon = 0.1$ and $\epsilon = 1$).

In the aim of robustness we therefore prefer the ILU method which is used in connection with the finite volume restriction and prolongation in all subsequent computations.

In addition, the different columns of these tables indicate that the results are essentially independent of the velocity direction (i.e. the angle α).

One of the main features of a multigrid method is that the convergence rate is uniformly bounded by some number smaller than 1. Our numerical experiments for problem 4.1

smoothing iteration	$\varepsilon \setminus \alpha$	$0°$	$15°$	$30°$	$45°$	$60°$	$75°$	$90°$	$135°$	$-45°$
ILU	1	.538	.538	.538	.538	.538	.538	.538	.542	.542
	0.1	.421	.429	.445	.455	.445	.429	.421	.457	.457
	0.01	.143	.136	.152	.157	.152	.136	.143	.190	.190
	0.001	.024	.008	.006	.007	.006	.008	.024	.014	.014
GS	0.1	.675	.695	.643	.633	.643	.695	.675	.634	.634
	0.01	.407	.370	.278	.221	.278	.371	.407	.285	.285
	0.001	.076	.044	.018	.016	.018	.044	.076	.032	.032
SOR ($\omega = 1.25$)	1	.921	.917	.914	.913	.914	.917	.921	.913	.913
	0.1	.557	.559	.546	.539	.546	.559	.557	.544	.544
	0.01	.226	.136	.110	.108	.108	.136	.226	.118	.118

Table 10: Petrov-Galerkin restriction and prolongation

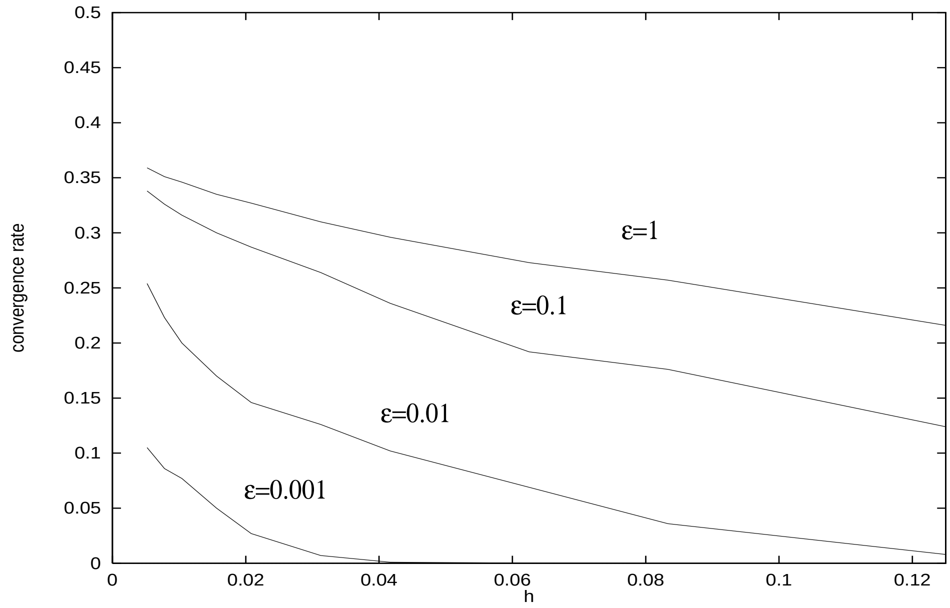

Figure 11: convergence rates for various diffusion parameters

with varying grid size h and different values of ϵ shown in figure 11 are confirming this property. For fixed grid size h the convergence rate is increasing in ϵ. The gap between the convergence rate for $\epsilon = 1$ and the other ones becomes smaller on finer grids. The uniform boundedness in h and – in the sense of robustness – even in ϵ is determined by the top line which seems to be bounded by 0.4.

In theorem 2.2 we have stated the convergence of order 2 in h and Δt. For the heat equation there should be no restriction on the coupling of h and Δt. In tables 12 and

$h\backslash\Delta t$	$\frac{1}{16}$	$\frac{1}{32}$	$\frac{1}{64}$	$\frac{1}{128}$
$\frac{1}{16}$	$3.03 \cdot 10^{-4}$	$1.66 \cdot 10^{-4}$	$1.04 \cdot 10^{-4}$	$8.87 \cdot 10^{-5}$
$\frac{1}{32}$	$2.42 \cdot 10^{-4}$	$1.03 \cdot 10^{-4}$	$4.11 \cdot 10^{-5}$	$2.58 \cdot 10^{-5}$
$\frac{1}{64}$	$2.27 \cdot 10^{-4}$	$8.72 \cdot 10^{-5}$	$2.53 \cdot 10^{-5}$	$1.01 \cdot 10^{-5}$
$\frac{1}{128}$	$2.24 \cdot 10^{-4}$	$8.32 \cdot 10^{-5}$	$2.14 \cdot 10^{-5}$	$6.13 \cdot 10^{-6}$

Table 12: Method of Gear with Euler Method as first step

$h\backslash\Delta t$	$\frac{1}{16}$	$\frac{1}{32}$	$\frac{1}{64}$	$\frac{1}{128}$
$\frac{1}{16}$	$9.17 \cdot 10^{-4}$	$2.91 \cdot 10^{-4}$	$1.36 \cdot 10^{-4}$	$9.69 \cdot 10^{-5}$
$\frac{1}{32}$	$8.54 \cdot 10^{-4}$	$2.29 \cdot 10^{-4}$	$7.28 \cdot 10^{-5}$	$3.34 \cdot 10^{-5}$
$\frac{1}{64}$	$8.38 \cdot 10^{-4}$	$2.13 \cdot 10^{-4}$	$5.70 \cdot 10^{-5}$	$1.82 \cdot 10^{-5}$
$\frac{1}{128}$	$8.34 \cdot 10^{-4}$	$2.09 \cdot 10^{-4}$	$5.32 \cdot 10^{-5}$	$1.43 \cdot 10^{-5}$

Table 13: Crank-Nicolson method

13 we have computed the error of the numerical solutions in the discrete ℓ_2-norm using the exact solution (34). These computations are in good agreement with the theoretical results. By a least square approximation for the error norm in the form

$$e(h, \Delta t) \approx C_1 h^2 + C_2 \Delta t^2$$

we have computed

$$\begin{array}{ll} C_1 = 0.0214\,, \quad C_2 = 0.0840 & \text{(method of Gear),} \\ C_1 = 0.0214\,, \quad C_2 = 0.2132 & \text{(Crank-Nicolson method).} \end{array}$$

The correspondence between the constants C_1 for both methods shows that the error can be splitted into a semidiscretization error and an error due to the time integrator. Better results are obtained for the method of Gear which has the smaller constant C_2.

In the convection problem 4.4 the initial condition is transported along the streamlines which are concentric circles. Here the initial 'hump' should be rotated with periodicity of 2π. Fig 11 shows the results with Gear and Crank-Nicolson method for one rotation at times $t = i\frac{\pi}{2}$, $i = 0, \ldots, 4$ on a 64×64-grid with 200 time steps. The height of the hump decreases about 3 % for the Gear method which is an effect of its damping behaviour. The shape of the hump is rotated by both methods without significant deformation or translation. The quality of these results is good in comparison with [8, 9].

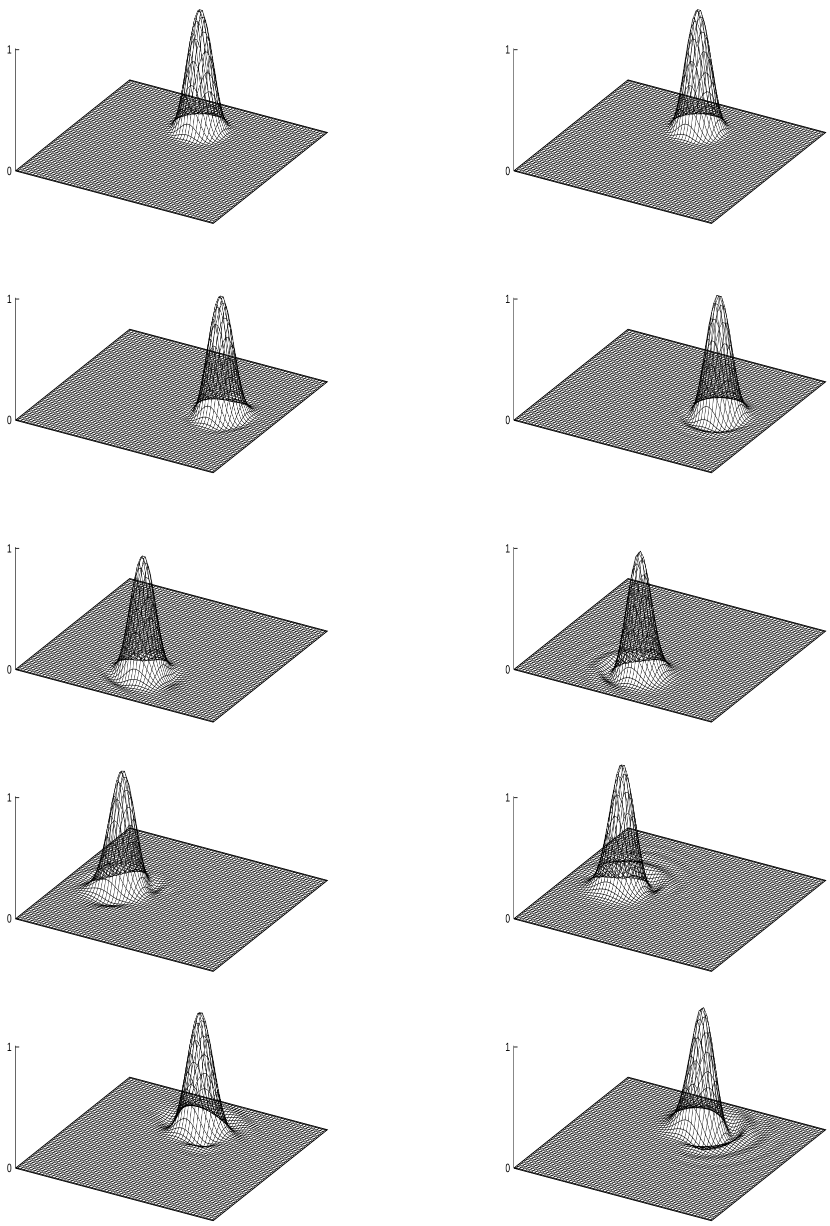

Figure 14: Different time integrators (Gear and Crank-Nicolson method)

5 Conclusion

We have presented a cell orientated semidiscretization for the convection-diffusion equation in two dimensions which is problem adapted and appropriate for convection dominated as well as diffusion dominated cases. The applicability in connection with implicit time integrators is mainly determined by the solution method for the linear systems.

A multigrid method for these systems was derived. The variant based on a finite volume interpretation for restriction and prolongation together with an ILU smoothing iteration turns out to be robust and very efficient.

References

[1] A. Brandt. *Guide to Multigrid Development.* In W. Hackbusch, U. Trottenberg, *Multigrid Methods I*, Lect. Notes Math., 220–312. Springer, Berlin 1982.

[2] K. E. Brenan, S. L. Campbell, L. R. Petzold. *Numerical Solution of Initial-Value Problems in Differential-Algebraic Equations.* North-Holland, New York 1989.

[3] W. Hackbusch. *Multi-Grid Methods and Applications*, Springer Ser. Comput. Math. 4. Springer, Berlin 1985.

[4] W. Hackbusch. *Iterative Solution of Large Sparse Systems of Equations*, Appl. Math. Sciences 95. Springer, New York 1994.

[5] D. Hietel. *Ein neuer Typ zellorientierter Diskretisierungsverfahren zur numerischen Lösung von Konvektions-Diffusions-Problemen.* Dissertation, Technische Hochschule Darmstadt 1991.

[6] V. P. Il'in. *Iterative Incomplete Factorization Methods.* World Scientific, Singapore 1992.

[7] R. Kornhuber, G. Wittum. *Discretization and Iterative Solution of Convection Diffusion Equations.* In W. Hackbusch, *Incomplete Decomposition (ILU) - Algorithms, Theory and Applications. Proceedings of the eighth GAMM-Seminar, Kiel*, Notes Numer. Fluid Mech. 41, 67–77. Vieweg, Wiesbaden 1993.

[8] W. J. Minkowycz, E. M. Sparrow, G. E. Schneider, R. H. Pletcher. *Handbook of Numerical Heat Transfer.* John Wiley & Sons, Chichester 1988.

[9] O. Pironneau. *Finite Element Methods for Fluids.* John Wiley & Sons, Chichester 1989.

[10] Y. Saad, M. H. Schultz. *GMRES: A generalized minimal residual algorithm for solving nonsymmetric linear systems.* SIAM J. Sci. Stat. Comput. **7** (1986) 856–869.

[11] R. M. Smith, A. G. Hutton. *The numerical treatment of advection: A performance comparison of current methods.* Numer. Heat Transfer **5** (1982) 439–461.

[12] P. Sonneveld. *CGS, a fast Lanczos-type solver for nonsymmetric linear systems.* SIAM J. Sci. Stat. Comput. **10** (1989) 36–52.

[13] P. Wesseling. *An Introduction to Multigrid Methods.* John Wiley & Sons, Chichester 1991.

[14] J. Witzel. *Präkonditionierte Petrov-Galerkin-Verfahren zur Lösung linearer Gleichungssysteme bei der Kopplung Finiter Methoden.* Diplomarbeit, Technische Hochschule Darmstadt 1992.